A Temperature-Based Formulation for Finite Element Analysis of Generalized Phase-Change Problems

D. Celentano
E. Oñate
S. Oller

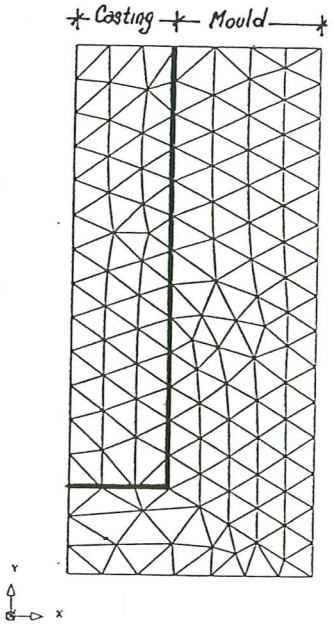

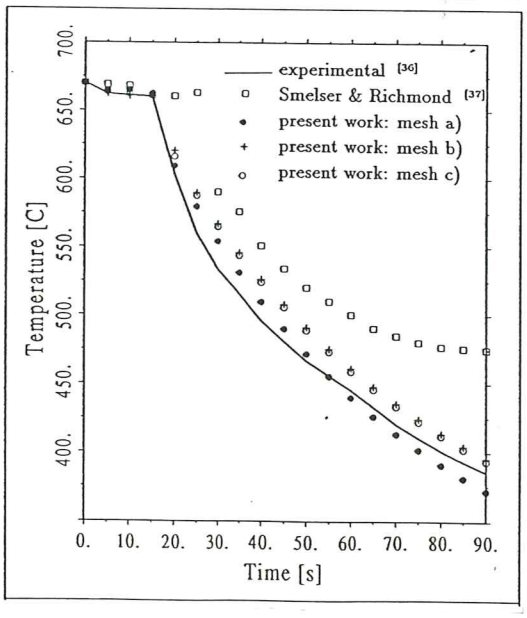

Publicación CIMNE Nº 28, Enero1993

A Temperature-Based Formulation for Finite Element Analysis of Generalized Phase-Change Problems

D. Celentano
E. Oñate
S.Oller

Publicación CIMNE Nº 28, Enero 1993

Centro Internacional de Métodos Numéricos en Ingeniería
Gran Capitán s/n, 08034 Barcelona, España

A TEMPERATURE-BASED FORMULATION FOR FINITE ELEMENT ANALYSIS OF GENERALIZED PHASE-CHANGE PROBLEMS

Diego Celentano - Eugenio Oñate - Sergio Oller

International Center for Numerical Methods in Engineering
E.T.S. d'Enginyers de Camins, Canals i Ports
Universitat Politècnica de Catalunya
Gran Capità s/n, Mòdul C1, 08034 Barcelona, Spain

SUMMARY.

A finite element formulation for solving multidimensional phase-change problems is presented. The formulation considers the temperature as the unique state variable, it is conservative in the weak form sense and it preserves the moving interface condition. In this work, a consistent Jacobian matrix that ensures numerical convergence and stability is derived. Also, a comparative analysis with other different phase-change finite element techniques is performed. Finally, two numerical examples are analyzed in order to show the performance of the proposed methodology.

1. INTRODUCTION.

Phase-change problems appear frequently in industrial processes and other problems of technological interest. The problem is highly non-linear due to the moving interface condition and, therefore, few analytical solutions can be obtained [1,2]. Numerical solutions employing finite differences [3–6], boundary elements [7,8], or finite elements [9–45] techniques have been attempted by many researchers.

Among the finite element procedures two important solution techniques are found: tracking and fixed-domain methods. The first one typically uses a deforming grid formulation in order to adapt the mesh to the interface displacements [14–19]. In this context, the energy interface equation is treated in a special form. Nevertheless, this method presents many drawbacks, such as the need of starting solutions for the front position and the difficulty of dealing with appearing/disappearing phases and multiple or no-smooth interfaces, as it has been reported in [42].

Fixed-domain methods are derived from a weak formulation that implicitly contains the moving interface condition. Within this framework, one option is to use the enthalpy as the main variable in order to take into account the latent heat effect. Once the nodal enthalpy vector is obtained for each time step, the nodal temperatures can be computed using the well-known enthalpy-temperature relationship. All enthalpy-based methods need a regularization to remove the discontinuity that appears at the phase-change front [20–34]. Rolph III and Bathe [35] and Roose and Storrer [36] use a fictitious heat source method based in the enthalpy concept. An alternative approach known as the source based method, also derived from the enthalpy concept, has been used by Reddy et al. [37]. Blanchard and Fremond [38] introduce the freezing index in the energy conservation equation and solve a variational equation with the help of an homographic approximation which contains an enthalpy regularization. Other transformation methods have developed by Ichikawa and Kikuchi [39] and Lee et al. [40].

Tamma and Railkar [41] employ the transfinite element technique in combination with the enthalpy method.

A second approach, exploited by Crivelli, Storti and Idelsohn [42–44], consists in retaining the temperature as the only state variable. In order to avoid any explicit smoothing, a special element able to integrate discontinuous functions must be used [42,43,45].

The objective of this paper is to present an alternative temperature-based finite element formulation. In Section 2 the governing equations for the isothermal (the standard Stefan's problem) and non-isothermal cases are presented. The weak form and the finite element formulation for the generalized phase-change problem are described in Section 3.

In order to achieve convergence and stability of the numerical solution, a new consistent Jacobian matrix is derived in Section 4.

A comparative analysis with other different techniques is performed in Section 5. Several crucial aspects of the proposed algorithm are also discussed. Section 6 includes two numerical examples showing a good agreement between analytical and numerical results obtained with the proposed methodology.

2. GOVERNING EQUATIONS.

Let an open bounded domain $\Omega \subset \mathbb{R}^{n_{dim}}$ $(1 \leq n_{dim} \leq 3)$ be the reference (initial) configuration of a non-linear heat conductor $\mathcal{B}_1$ with particles defined by $\boldsymbol{x} \in \bar{\Omega}$, $\Gamma = \partial\Omega$ its smooth boundary and $\Upsilon \subset \mathbb{R}^+$ be the time interval of analysis $(t \in \Upsilon)$. As usual, $\bar{\Omega} = \Omega \cup \Gamma$. The standard Stefan's problem [1,2] consists in finding an absolute temperature field $T : \bar{\Omega} \times \Upsilon \rightarrow \mathbb{R}^+$ such that,

$$\rho_o \frac{\partial \omega}{\partial T} \dot{T} = -div[\boldsymbol{q}] + \rho_o \, r \qquad in: \ \Omega_s \times \Upsilon \ and \ \Omega_l \times \Upsilon \ , \tag{2.1.a-b}$$

$$\boldsymbol{q} = \hat{\boldsymbol{q}}(\boldsymbol{x}, t) \qquad in \ \Omega \times \Upsilon \ , \tag{2.2}$$

$$c = \frac{\partial \omega}{\partial T} \qquad in \ \Omega \times \Upsilon \ , \tag{2.3}$$

subject to the boundary conditions,

$$T = \bar{T} \qquad in \ \Gamma_T \times \Upsilon \ , \tag{2.4}$$

$$\boldsymbol{q} \cdot \boldsymbol{n} = -\bar{q} - q_{conv} \qquad in \ \Gamma_q \times \Upsilon \ , \tag{2.5}$$

the initial condition,

$$T(\boldsymbol{x}, t)|_{t=0} = T_o(\boldsymbol{x}) \quad in \ \Omega \ , \tag{2.6}$$

and the energy equation at the moving interface $\Gamma_{pc} \subset \mathbb{R}^{n_{dim}-1}$ which separates the solid and liquid phases (denoted by subscripts s and l respectively):

$$q_s \cdot n_s + q_l \cdot n_l = \rho_o \, L \, \dot{\boldsymbol{x}} \cdot \boldsymbol{n}_l \qquad in \ \Gamma_{pc} \times \Upsilon \ \ and \ \ T = T_m. \tag{2.7}$$

Equation (2.1) is the energy balance derived from the First Law of Thermodynamics (neglecting mechanical effects and volume changes [46,48]) where the dot denotes time derivative, and the symbol *div* denotes the divergence operator relative to a Cartesian reference system. $\rho_o : \Omega \rightarrow \mathbb{R}^+$ is the density at the reference configuration, $\omega : \Omega \times \Upsilon \rightarrow \mathbb{R}$ the specific internal energy (per unit mass), $r : \Omega \times \Upsilon \rightarrow \mathbb{R}$ the specific heat source, $q : \bar{\Omega} \times \Upsilon \rightarrow \mathbb{R}^{n_{dim}}$ the heat flux vector and equation (2.2) represents its constitutive law. The superposed caret in $\hat{q}$ serves to distinguish this function from its value. Equation (2.3) is the standard definition of the specific heat capacity $c : \Omega \times \Upsilon \rightarrow \mathbb{R}^+$. It is worth noting that c may be temperature dependent.

At any time t, Ω can be decomposed into two subdomains ($\Omega_s \subset \mathbb{R}^{n_{dim}}$ and $\Omega_l \subset \mathbb{R}^{n_{dim}}$) such that $x \in \Omega_s$ *if* $T(x,t) < T_m$ (solid phase) and $x \in \Omega_l$ *if* $T(x,t) > T_m$ (liquid phase), with the following properties:

$$\bar{\Omega}_s \cup \bar{\Omega}_l = \bar{\Omega} \ , \tag{2.8.a}$$

$$\Omega_s \cap \Omega_l = \emptyset \ , \tag{2.8.b}$$

and

$$\Omega_s \cup \Omega_l \cup \Gamma_{pc} = \Omega \ , \tag{2.8.c}$$

$$\bar{\Omega}_s \cap \bar{\Omega}_l = \bar{\Gamma}_{pc} \ , \tag{2.8.d}$$

where T_m is the melting temperature at the interface Γ_{pc} (see *Figure* 1).

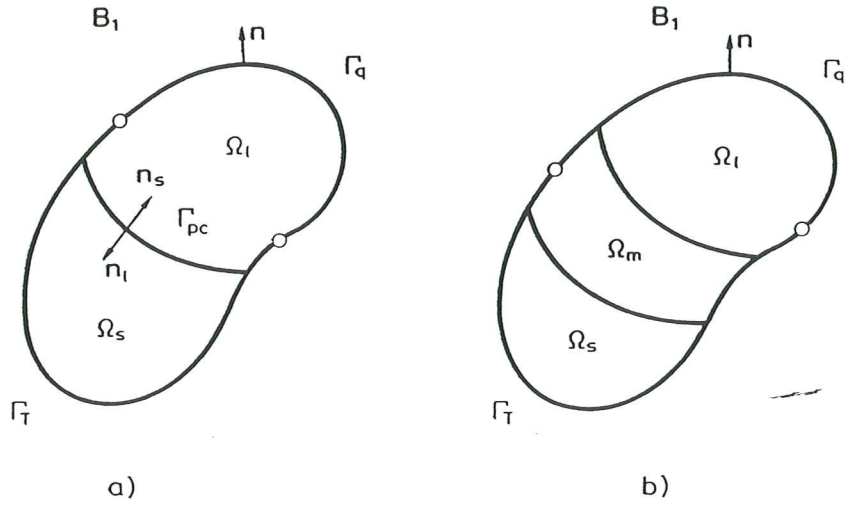

Figure 1. Geometric description of a non-linear heat conductor $\mathcal{B}_1$ for phase-change problems: a) isothermal case. b) non-isothermal case.

In equation (2.4), $\Gamma_T \subset \mathbb{R}^{n_{dim}-1}$ is the part of the boundary where the temperature $\bar{T} : \Gamma_T \times \Upsilon \rightarrow \mathbb{R}^+$ is prescribed (Dirichlet boundary condition), while in equation (2.5) (written in standard tensor notation [50]), $\Gamma_q \subset \mathbb{R}^{n_{dim}-1}$,with unit outward normal $n : \partial\Omega \rightarrow S^{n_{dim}-1}$, is the region where the normal heat flux is applied: a) $\bar{q} : \Gamma_q \times \Upsilon \rightarrow \mathbb{R}$ is the prescribed normal heat flux and b) $q_{conv} : \Gamma_q \times \Upsilon \rightarrow \mathbb{R}$ is the normal heat flux due to

convection-radiation phenomena. For this last term, the standard Newton's constitutive law is adopted:

$$q_{conv} = -h\,(T - T_{env})\ , \tag{2.9}$$

where $h : \Gamma_q \times \Upsilon \rightarrow \mathbb{R}^+$ is the convection-radiation coefficient (temperature dependent) and $T_{env} : \bar{\Omega}_{out} \times \Upsilon \rightarrow \mathbb{R}^+$ is the environmental temperature (defined outside Ω). In a general case, T_{env} is the temperature at the boundary of another body $\mathcal{B}_2$, and equation (2.9) is the constitutive law of the medium that separates both bodies.

The boundary condition (2.5) is of mixed type, but becomes of Neumann type when $q_{conv} = 0$. As usual, the conditions

$$\bar{\Gamma}_T \cup \bar{\Gamma}_q = \partial\bar{\Omega}\ , \tag{2.10.a}$$

and

$$\Gamma_T \cap \Gamma_q = \emptyset\ , \tag{2.10.b}$$

are assumed to hold.

In equation (2.7), L is the latent heat released in a freezing problem (or absorbed in a melting one) with $T = T_m$ in Γ_{pc}, and $\dot{\boldsymbol{x}}(\boldsymbol{x},t) : \Gamma_{pc} \times \Upsilon \rightarrow \mathbb{R}^{n_{dim}}$ is the interface velocity. Considering only Ω_s, the outward unit normal to the interface is denoted by $\boldsymbol{n}_s : \partial\Gamma_{pc} \rightarrow S^{n_{dim}-1}$, while $\boldsymbol{q}_s : \partial\Gamma_{pc} \times \Upsilon \rightarrow \mathbb{R}^{n_{dim}}$ is the heat flux vector existing at points $\boldsymbol{x} \in \Gamma_{pc}$. Similar definitions of $\boldsymbol{n}_l$ and $\boldsymbol{q}_l$ are obtained when considering only Ω_l. Obviously, at a point $\boldsymbol{x} \in \Gamma_{pc}$, $\boldsymbol{n}_l = -\boldsymbol{n}_s$. Equation (2.7) shows that the heat flux presents a discontinuity across the moving interface. This fact makes the problem highly non-linear.

For a full description of the problem, an appropriate constitutive law for $\boldsymbol{q}$ (equation (2.3)) is necessary. The well-known Fourier's law is adopted:

$$\boldsymbol{q} = \hat{\boldsymbol{q}}(\boldsymbol{x},t) = -\boldsymbol{k}\cdot\nabla T \qquad in\ \Omega\times\Upsilon\ , \tag{2.11}$$

where $\boldsymbol{k} : \Omega \times \Upsilon \rightarrow \mathbb{R}^{n_{dim}} \times \mathbb{R}^{n_{dim}}$ is the conductivity second-rank tensor (which may be temperature dependent) and $\nabla(\cdot) = \frac{\partial(\cdot)}{\partial \boldsymbol{x}}$ is the gradient operator. As a consequence of the Second Law of Thermodynamics, this tensor must be positive semidefinite [46].

This path independent way of defining $\boldsymbol{q}$ is equivalent to that used by Simo [47] in terms of a heat flux potential $\mathcal{H} : \Omega \times \mathbb{R}^{n_{dim}} \rightarrow \mathbb{R}$ (depending on the position and the temperature gradient) that is a smooth convex function for all $\boldsymbol{x} \in \Omega$ such that,

$$\boldsymbol{q} = \hat{\boldsymbol{q}}(\boldsymbol{x},t) = -\bar{\nabla}\mathcal{H}(\boldsymbol{x},\nabla T(\boldsymbol{x},t)) \qquad in\ \Omega\times\Upsilon\ , \tag{2.12}$$

with

$$\mathcal{H}(\boldsymbol{x},\nabla T(\boldsymbol{x},t)) = \frac{1}{2}\,\nabla T\cdot\boldsymbol{k}\cdot\nabla T \qquad in\ \Omega\times\Upsilon\ , \tag{2.13}$$

where $\bar{\nabla}(\cdot) = \frac{\partial(\cdot)}{\partial\nabla T}$ (in components, $\bar{\nabla}_i(\cdot) = \frac{\partial(\cdot)}{\partial T_{,i}}$).

When the latent heat is released (or absorbed) in a range of temperatures $(T_l - T_s)$, with T_s and T_l being the solidus and liquidus temperatures respectively, the governing equations (with the notation described above) are:

$$\rho_o \frac{\partial \omega}{\partial T} \dot{T} = -div[\boldsymbol{q}] + \rho_o \, r \qquad in: \ \Omega_s \times \Upsilon, \ \Omega_m \times \Upsilon \ and \ \Omega_l \times \Upsilon \ , \tag{2.14.a-b-c}$$

$$\boldsymbol{q} = \hat{\boldsymbol{q}}(\boldsymbol{x}, t) \qquad in \ \Omega \times \Upsilon \ , \tag{2.15}$$

where in this case the temperature derivative of the specific internal energy takes the form:

$$c + L \frac{\partial f(T)}{\partial T} = \frac{\partial \omega}{\partial T} \qquad in \ \Omega \times \Upsilon \ , \tag{2.16}$$

subjected to the same boundary and initial conditions described above (equations (2.4), (2.5) and (2.6)).

Now, at any time t, Ω can be decomposed into three subdomains ($\Omega_s \subset \mathbb{R}^{n_{dim}}$, $\Omega_m \subset \mathbb{R}^{n_{dim}}$ and $\Omega_l \subset \mathbb{R}^{n_{dim}}$), such that $\boldsymbol{x} \in \Omega_s$ *if* $T(\boldsymbol{x}, t) < T_s$ (solid phase), $\boldsymbol{x} \in \Omega_m$ *if* $T_s \leq T(\boldsymbol{x}, t) \leq T_l$ (mushy phase) and, $\boldsymbol{x} \in \Omega_l$ *if* $T(\boldsymbol{x}, t) > T_l$ (liquid phase), with the property (see *Figure* 1):

$$\bar{\Omega}_s \cup \bar{\Omega}_m \cup \bar{\Omega}_l = \bar{\Omega} \ , \tag{2.17.a}$$

$$\Omega_s \cap \Omega_m \cap \Omega_l = \emptyset \ , \tag{2.17.b}$$

$$\Omega_s \cup \Omega_m \cup \Omega_l = \Omega \ , \tag{2.17.c}$$

In equation (2.16) f is defined as:

$$f(T) \ = \ \begin{cases} 0 & ; \forall \ T < T_s \\ 0 \leq g(T) \leq 1 & ; T_s \leq \forall \ T \leq T_l \\ 1 & ; \forall \ T > T_l . \end{cases} \tag{2.18}$$

The function $g(T)$ may be obtained using a microstructure model [31]. However, from a macroscopical point of view assumed in this paper, the simplest choice for $g(T)$ is the linear one with:

$$g(T) = (T - T_s)/(T_l - T_s) \quad ; \forall \ T_s \leq T \leq T_l . \tag{2.19}$$

It can be observed that the latent heat effect appears in Ω_m. In Ω_s and Ω_l, the classical definition of c (equation (2.3)) is recovered because the temperature derivative of f is zero in those regions. Therefore, equations (2.14) can be written as:

$$\rho_o \, (c \ + L \frac{\partial f}{\partial T}) \, \dot{T} = -div[\boldsymbol{q}] + \rho_o \, r \qquad in \ \Omega \times \Upsilon \ , \tag{2.20}$$

or

$$\rho_o \, c \, \dot{T} + \rho_o \, L \, \dot{f} = -div[\boldsymbol{q}] + \rho_o \, r \qquad in \ \Omega \times \Upsilon . \tag{2.21}$$

3. WEAK FORM AND FINITE ELEMENT FORMULATION.

In order to obtain the weak form of this initial boundary value problem, a space $\mathcal{V}$ of admissible test functions is defined as:

$$\mathcal{V} = \left\{ \eta \in H^1(\Omega) \mid \eta = 0 \ on \ \Gamma_T \right\} , \tag{3.1}$$

where $H^1(\Omega)$ is the standard notation for the Sobolev space [47].

An admissible solution space ${}^t\mathcal{L}$ (for fixed time $t \in \Upsilon$) is given by:

$${}^t\mathcal{L} = \left\{ T(\boldsymbol{x},t) \in H^1(\Omega) \mid T(\boldsymbol{x},t) = \bar{T}(\boldsymbol{x},t) \ on \ \Gamma_T \right\}. \tag{3.2}$$

The integral problem for the isothermal case can be formulated as: find a temperature field $T(\boldsymbol{x},t)$ that satisfies the corresponding equations for this case (equations (2.1) to (2.7)), such that:

$$\begin{aligned} &-\langle \rho_o \, c \, \dot{T}, \eta \rangle_{\Omega_s} - \langle div[\boldsymbol{q}], \eta \rangle_{\Omega_s} + \langle \rho_o \, r, \eta \rangle_{\Omega_s} - \\ &-\langle \rho_o \, c \, \dot{T}, \eta \rangle_{\Omega_l} - \langle div[\boldsymbol{q}], \eta \rangle_{\Omega_l} + \langle \rho_o \, r, \eta \rangle_{\Omega_l} + \\ &+\langle \boldsymbol{q} \cdot \boldsymbol{n}, \eta \rangle_{\Gamma_q} + \langle \bar{q}, \eta \rangle_{\Gamma_q} + \langle q_{conv}, \eta \rangle_{\Gamma_q} - \\ &-\langle \boldsymbol{q}_s \cdot \boldsymbol{n}_s, \eta \rangle_{\Gamma_{pc}} - \langle \boldsymbol{q}_l \cdot \boldsymbol{n}_l, \eta \rangle_{\Gamma_{pc}} + \langle \rho_o \, L \, \dot{\boldsymbol{x}} \cdot \boldsymbol{n}_l, \eta \rangle_{\Gamma_{pc}} = 0 \qquad \forall \eta \in \mathcal{V} , \end{aligned} \tag{3.3}$$

with the initial condition:

$$\langle T(\boldsymbol{x},0), \eta \rangle = \langle T_o, \eta \rangle \qquad \forall \eta \in \mathcal{V} , \tag{3.4}$$

where $\langle \cdot, \cdot \rangle_{\Omega_s}$, $\langle \cdot, \cdot \rangle_{\Omega_l}$, $\langle \cdot, \cdot \rangle_{\Gamma_q}$ and $\langle \cdot, \cdot \rangle_{\Gamma_{pc}}$ denotes the standard L_2-pairing in Ω_s, Ω_l, $\partial\Omega$ and Γ_{pc} respectively ($L_2(\Omega)$ being the Hilbert space of square integrable functions on Ω).

Similarly for the non-isothermal case (equation (2.21)), it follows that:

$$\begin{aligned} &-\langle \rho_o \, c \, \dot{T}, \eta \rangle_{\Omega} - \langle \rho_o \, L \, \dot{f}, \eta \rangle_{\Omega} - \langle div[\boldsymbol{q}], \eta \rangle_{\Omega} + \langle \rho_o \, r, \eta \rangle_{\Omega} + \\ &+\langle \boldsymbol{q} \cdot \boldsymbol{n}, \eta \rangle_{\Gamma_q} + \langle \bar{q}, \eta \rangle_{\Gamma_q} + \langle q_{conv}, \eta \rangle_{\Gamma_q} = 0 \qquad \forall \eta \in \mathcal{V} , \end{aligned} \tag{3.5}$$

again, with equation (3.4) as the initial condition.

After some mathematical manipulations, keeping in mind the initial condition, both isothermal and non-isothermal cases may be summarized as [51–54]:

$$\begin{aligned} &-\langle \rho_o \, c \, \dot{T}, \eta \rangle_{\Omega} - \langle \rho_o \, L \, \dot{f}_{pc}, \eta \rangle_{\Omega} - \langle div[\boldsymbol{q}], \eta \rangle_{\Omega} + \langle \rho_o \, r, \eta \rangle_{\Omega} + \\ &+\langle \boldsymbol{q} \cdot \boldsymbol{n}, \eta \rangle_{\Gamma_q} + \langle \bar{q}, \eta \rangle_{\Gamma_q} + \langle q_{conv}, \eta \rangle_{\Gamma_q} = 0 \qquad \forall \eta \in \mathcal{V} , \end{aligned} \tag{3.6}$$

and with $f_{pc} = H(T - T_m)$ being the Heaviside function for the isothermal case, and $f_{pc} = f(T)$ for the non-isothermal one (see *Figure* 2). The Heaviside function is defined as:

$$H(T - T_m) = \begin{cases} 0 & ; \forall \ T \leq T_m \\ 1 & ; \forall \ T > T_m . \end{cases} \tag{3.7}$$

Equations (3.6) and (3.4) describe the generalized phase-change problem in integral form. A further generalization takes place when two or more phase-changes ($n_{pc} \geq 2$) occur. For this case, the term $L\ \dot{f}_{pc}$ must be replaced by $\sum_{i=1}^{n_{pc}} L_i\ \dot{f}_{pc_i}$ (L_i and f_{pc_i} are the latent heat and the phase-change function associated with the i-th phase-change, respectively) in equation (3.6) and subsequents equations derived in this and next Sections. For simplicity in the notation, the simpler form of equation (3.6) is retained.

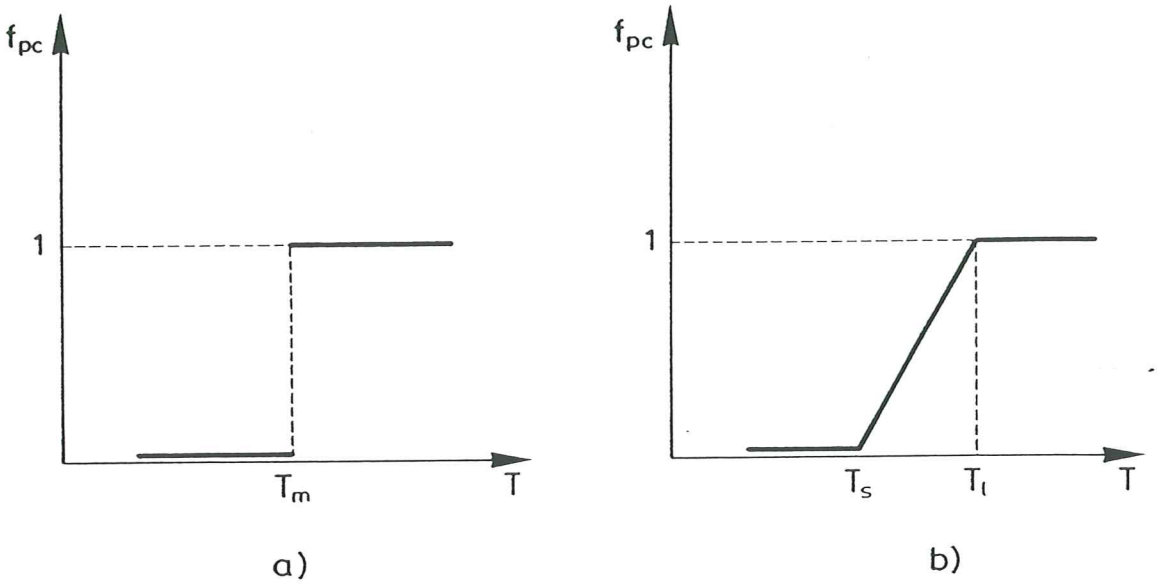

Figure 2. Phase-change function for: a) isothermal case. b) non-isothermal case.

Different authors [20–45] formulate the general problem starting from equation (2.20) as:

$$-\langle \rho_o\ (c + L\ \frac{\partial f_{pc}}{\partial T})\ \dot{T}, \eta \rangle_\Omega - \langle div[q], \eta \rangle_\Omega + \langle \rho_o\ r, \eta \rangle_\Omega +$$

$$+\langle q \cdot n, \eta \rangle_{\Gamma_q} + \langle \bar{q}, \eta \rangle_{\Gamma_q} + \langle q_{conv}, \eta \rangle_{\Gamma_q} = 0 \qquad \forall \eta \in \mathcal{V}. \tag{3.8}$$

It should be noted that in the isothermal case, the temperature derivative of f_{pc} is equal to $\delta(T - T_m)$ (Dirac function). For numerical reasons to be discussed in Section 5, the integral equation (3.6) (instead of (3.8)) will be used in this and subsequents Sections.

An important advantage that appears when standard mathematical arguments are used for equation (3.6) is that the local form of the equations for the generalized phase-change problem can be derived. These are formally identical to the equations corresponding to the non-isothermal case, but considering f_{pc} instead of f.

To integrate in time equation (3.6), a generalized mid-point rule algorithm can be used [47]. Let $[t, t + \Delta t] \subset \Upsilon$ ($\Delta t > 0$) be a time subinterval. Assuming that at time t an algorithmic approximations of the temperature ${}^tT(\boldsymbol{x}) : \Omega \rightarrow \mathbb{R}^+$ and temperature rate ${}^t\dot{T}(\boldsymbol{x}) : \Omega \rightarrow \mathbb{R}$ are known, the objective is to obtain ${}^{t+\Delta t}T(\boldsymbol{x})$ and ${}^{t+\Delta t}\dot{T}(\boldsymbol{x})$ at time $t + \Delta t$. To this end, it is necessary to find ${}^{t+\Delta t}T$ which verifies equations (2.1) to (2.7) or (2.14) to (2.16) in the isothermal or non-isothermal phase-change problem respectively, such that:

$$-\langle \rho_o \, {}^{t+\alpha\Delta t}c \, {}^{t+\alpha\Delta t}\dot{T}, \eta\rangle_\Omega - \langle \rho_o \, L \, {}^{t+\alpha\Delta t}\dot{f}_{pc}, \eta\rangle_\Omega - \langle div[{}^{t+\alpha\Delta t}\boldsymbol{q}], \eta\rangle_\Omega + \langle \rho_o \, {}^{t+\alpha\Delta t}r, \eta\rangle_\Omega +$$

$$+\langle {}^{t+\alpha\Delta t}\boldsymbol{q}\cdot\boldsymbol{n}, \eta\rangle_{\Gamma_q} + \langle {}^{t+\alpha\Delta t}\bar{q}, \eta\rangle_{\Gamma_q} + \langle {}^{t+\alpha\Delta t}q_{conv}, \eta\rangle_{\Gamma_q} = 0 \qquad \forall \eta \in \mathcal{V} \,, \qquad (3.9)$$

where

$${}^{t+\alpha\Delta t}\dot{\mathcal{X}} = (\, {}^{t+\Delta t}\mathcal{X} - \, {}^{t}\mathcal{X})/\Delta t \,, \qquad (3.10.a)$$

$${}^{t+\alpha\Delta t}\mathcal{X} = \alpha \, {}^{t+\Delta t}\mathcal{X} + (1-\alpha) \, {}^{t}\mathcal{X} \qquad with \; \alpha \in [0,1] \,, \qquad (3.10.b)$$

$\mathcal{X}$ being any variable with superscript $t+\alpha\Delta t$ in equation (3.9). Again, as in equation (3.6), both isothermal and non-isothermal problems are summarized in equation (3.9).

Choosing $\alpha = 1$ (the well-known Euler backward method), inconditional stability is achieved [47,49].

In the context of the finite element technique [49,55], the discrete problem can be obtained via a spatial Galerkin projection of the continuum problem into a finite dimensional subspace ${}_h\mathcal{V} \subset \mathcal{V}$ of admissible C^o continuous shape functions defined as:

$${}_h\mathcal{V} = \left\{ N \in H^1(\Omega) \mid N = 0 \; on \; \Gamma_T \right\}. \qquad (3.11)$$

Consequently, an admissible "algorithmic" solution space ${}^t_h\mathcal{L} \subset {}^t\mathcal{L}$ (for fixed time $t \in \Upsilon$) is given by:

$${}^t_h\mathcal{L} = \left\{ \, {}^t_hT(\boldsymbol{x}) \in H^1(\Omega) \mid {}^t_hT(\boldsymbol{x}) = \, {}^t\bar{T}(\boldsymbol{x}) \; on \; \Gamma_T \right\} \,, \qquad (3.12)$$

also consisting of typical C^o functions [55].

Then, the discretized problem is written as:

$$-\langle \rho_o \, {}^{t+\Delta t}c \, {}^{t+\Delta t}_h\dot{T}, N\rangle_\Omega - \langle \rho_o \, L \, {}^{t+\Delta t}_h\dot{f}_{pc}, N\rangle_\Omega - \langle div[{}^{t+\Delta t}_h\boldsymbol{q}], N\rangle_\Omega + \langle \rho_o \, {}^{t+\Delta t}r, N\rangle_\Omega +$$

$$+\langle {}^{t+\Delta t}_h\boldsymbol{q}\cdot\boldsymbol{n}, N\rangle_{\Gamma_q} + \langle {}^{t+\Delta t}\bar{q}, N\rangle_{\Gamma_q} + \langle {}^{t+\Delta t}_h q_{conv}, N\rangle_{\Gamma_q} = 0 \qquad \forall N \in {}_h\mathcal{V}. \qquad (3.13)$$

Making use of the standard spatial interpolation for the temperature field [49], it leads to:

$${}^t_hT(\boldsymbol{x}) = \boldsymbol{N}^{(e)}(\boldsymbol{x}) \, {}^t_h\boldsymbol{T}^{(e)} \qquad with \; N_i^{(e)} \in {}_h\mathcal{V} \quad (i = 1, n_{node}), \; and \; e = 1, n_{elem} \; ; \qquad (3.14)$$

where $\boldsymbol{N}^{(e)}$ is the shape function matrix $(1 \times n_{node})$ and ${}^t_h\boldsymbol{T}^{(e)}$ is the nodal temperature vector at element e. For simplicity in the notation, the subscript h will be dropped from here onwards.

Following standard procedures, the global discretized thermal equilibrium equations can be written in matrix form as:

$$ {}^{t+\Delta t}F - {}^{t+\Delta t}C\ {}^{t+\Delta t}\dot{T} - {}^{t+\Delta t}K\ {}^{t+\Delta t}T - {}^{t+\Delta t}\dot{L} = 0 \ , \qquad (3.15) $$

where F is the external heat flux vector, C is the capacity matrix, K is the conductivity matrix and $\dot{L}$ is the "phase-change" vector rate. As usual, all vectors and matrices are assembled from the element contributions in the standard manner [49]. The form of the different elemental expressions appearing in equation (3.15) can be seen in Box 1, where the superscript $\mathcal{T}$ denotes the transpose symbol, F_c represents the concentrated heat flux vector (temperature-dependent in a general case), and n_c is the number of loaded nodes at element e. The term $\dot{L}$ contains the latent heat effect when $\dot{f}_{pc} \neq 0$.

Using an Euler-backward approximation of the time derivatives, equation (3.15) yields:

$$ {}^{t+\Delta t}R = {}^{t+\Delta t}F - \left[\frac{{}^{t+\Delta t}C}{\Delta t} + {}^{t+\Delta t}K\right] {}^{t+\Delta t}T + \frac{{}^{t+\Delta t}C}{\Delta t}\,{}^{t}T - \frac{{}^{t+\Delta t}L}{\Delta t} + \frac{{}^{t}L}{\Delta t} = 0 \ , \qquad (3.16) $$

where R is the residual vector and the element contributions of L at times t and $t+\Delta t$ can also be seen in Box 1.

4. SOLUTION STRATEGY.

When the residual is differentiable, an incremental iterative formulation for solving the non-linear system of equations (3.16) can be attempted. This means that [49]:

$$ {}^{t+\Delta t}R^{j} = {}^{t+\Delta t}R^{j-1} + \frac{\partial\ {}^{t+\Delta t}R^{j-1}}{\partial\ {}^{t+\Delta t}T^{j-1}}\ \Delta T^{j} = 0 \ , \qquad (4.1) $$

where the iteration index j denotes the j-th approximation to the solution in $t+\Delta t$. Therefore, the incremental iterative system can be written as:

$$ {}^{t+\Delta t}J^{j-1}\ \Delta T^{j} = {}^{t+\Delta t}R^{j-1} \ , \qquad (4.2) $$

$$ {}^{t+\Delta t}T^{j} = {}^{t+\Delta t}T^{j-1} + \Delta T^{j} \qquad j = 1, ..., n_{iter} \ ; \qquad (4.3.a) $$

$$ {}^{t+\Delta t}T^{o} = {}^{t}T \ , \qquad (4.3.b) $$

with the tangent Jacobian matrix (for iteration j) given by:

Box 1

Element matrices and vectors in the discretized thermal equilibrium equations.

$$
\begin{aligned}
{}^{t+\Delta t}\boldsymbol{F}^{(e)} &= \int_{\Omega^{(e)}} \boldsymbol{N}^{(e)\mathcal{T}}\, \rho_o\, {}^{t+\Delta t}\boldsymbol{r}\, d\Omega + \int_{\Gamma_q^{(e)}} \boldsymbol{N}^{(e)\mathcal{T}} \cdot {}^{t+\Delta t}\bar{q}\, d\Gamma_q + \\
&+ \int_{\Gamma_q^{(e)}} \boldsymbol{N}^{(e)\mathcal{T}}\, {}^{t+\Delta t}h\, {}^{t+\Delta t}T_{env}\, d\Gamma_q + \sum_{i=1}^{n_c} {}^{t+\Delta t}\boldsymbol{F}_{c_i}^{(e)} \\
{}^{t+\Delta t}\boldsymbol{C}^{(e)} &= \int_{\Omega^{(e)}} \boldsymbol{N}^{(e)\mathcal{T}}\, \rho_o\, {}^{t+\Delta t}c\ \boldsymbol{N}^{(e)}\, d\Omega \\
{}^{t+\Delta t}\boldsymbol{K}^{(e)} &= \int_{\Omega^{(e)}} (\nabla \boldsymbol{N}^{(e)})^{\mathcal{T}}\, {}^{t+\Delta t}\boldsymbol{k}\, (\nabla \boldsymbol{N}^{(e)})\, d\Omega + \int_{\Gamma_q^{(e)}} \boldsymbol{N}^{(e)\mathcal{T}}\, {}^{t+\Delta t}h\, \boldsymbol{N}^{(e)}\, d\Gamma_q \\
{}^{t+\Delta t}\dot{\boldsymbol{L}}^{(e)} &= \int_{\Omega^{(e)}} \boldsymbol{N}^{(e)\mathcal{T}}\, \rho_o\, L\ {}^{t+\Delta t}\dot{f}_{pc}\, d\Omega = \frac{{}^{t+\Delta t}\boldsymbol{L}^{(e)}}{\Delta t} - \frac{{}^{t}\boldsymbol{L}^{(e)}}{\Delta t}
\end{aligned}
$$

with

$$
\begin{aligned}
{}^{t}\boldsymbol{L}^{(e)} &= \int_{\Omega^{(e)}} \boldsymbol{N}^{(e)\mathcal{T}}\, \rho_o\, L\ {}^{t}f_{pc}\, d\Omega \\
{}^{t+\Delta t}\boldsymbol{L}^{(e)} &= \int_{\Omega^{(e)}} \boldsymbol{N}^{(e)\mathcal{T}}\, \rho_o\, L\ {}^{t+\Delta t}f_{pc}\, d\Omega
\end{aligned}
$$

$$
{}^{t+\Delta t}\boldsymbol{J}^{j} = -\frac{\partial\, {}^{t+\Delta t}\boldsymbol{R}^{j}}{\partial\, {}^{t+\Delta t}\boldsymbol{T}^{j}}. \tag{4.4}
$$

Replacing equation (3.16) into (4.4), the later becomes:

$$
{}^{t+\Delta t}\boldsymbol{J}^{j} = {}^{t+\Delta t}\boldsymbol{K}^{j} + \frac{{}^{t+\Delta t}\boldsymbol{C}^{j}}{\Delta t} + \frac{{}^{t+\Delta t}\boldsymbol{C}_{pc}^{j}}{\Delta t} + {}^{t+\Delta t}\boldsymbol{K}_{td}^{j} + \frac{{}^{t+\Delta t}\boldsymbol{C}_{td}^{j}}{\Delta t} - {}^{t+\Delta t}\boldsymbol{E}^{j}. \tag{4.5}
$$

The element contributions of $\boldsymbol{C}_{pc}$, $\boldsymbol{K}_{td}$, $\boldsymbol{C}_{td}$ and $\boldsymbol{E}$ are shown in **Box 2**.

$\boldsymbol{C}_{pc}$ is called the "phase-change" matrix, while the "td" matrices appear because of the temperature-dependent thermal properties (c, k_{ij} and h are assumed to be smooth functions of T). Note that the first term of $\boldsymbol{K}_{td}$ is non-symmetric. Finally, matrix $\boldsymbol{E}$ is due to temperature-dependent external actions (also assumed to be smooth functions of T).

It can be observed in **Box 2** that the Jacobian matrix exists if the same occurs with all the temperature derivatives appearing in such equations. Clearly, this is not the case with f_{pc} in the isothermal case (as mentioned above, which results in a Dirac function). Nevertheless, an approximated numerical smoothing can be performed in order to avoid this discontinuity. One possibility is:

$$
\left.\frac{\partial\, {}^{t+\Delta t}f_{pc}}{\partial\, {}^{t+\Delta t}T}\right|^{j} = \frac{{}^{t+\Delta t}f_{pc}^{j} - {}^{t+\Delta t}f_{pc}^{j-1}}{{}^{t+\Delta t}T^{j} - {}^{t+\Delta t}T^{j-1}}. \tag{4.6}
$$

Box 2

Element matrices appearing in the Jacobian matrix.

$$
\begin{aligned}
{}^{t+\Delta t}\boldsymbol{C}_{pc}^{(e)} &= \int_{\Omega^{(e)}} \boldsymbol{N}^{(e)\mathcal{T}}\, \rho_o\, L\, \frac{\partial\, {}^{t+\Delta t}f_{pc}}{\partial\, {}^{t+\Delta t}T}\, \boldsymbol{N}^{(e)}\, d\Omega \\
{}^{t+\Delta t}\boldsymbol{K}_{td}^{(e)} &= \int_{\Omega^{(e)}} (\nabla\, \boldsymbol{N}^{(e)})^{\mathcal{T}}\, \frac{\partial\, {}^{t+\Delta t}\boldsymbol{k}}{\partial\, {}^{t+\Delta t}T}\, (\nabla\, \boldsymbol{N}^{(e)})\; {}^{t+\Delta t}\boldsymbol{T}^{(e)}\; \boldsymbol{N}^{(e)}\, d\Omega + \\
&\quad + \int_{\Gamma_q^{(e)}} \boldsymbol{N}^{(e)\mathcal{T}}\, \frac{\partial\, {}^{t+\Delta t}h}{\partial\, {}^{t+\Delta t}T}\; {}^{t+\Delta t}T\; \boldsymbol{N}^{(e)}\, d\Gamma_q \\
{}^{t+\Delta t}\boldsymbol{C}_{td}^{(e)} &= \int_{\Omega^{(e)}} \boldsymbol{N}^{(e)\mathcal{T}}\, \rho_o\, \frac{\partial\, {}^{t+\Delta t}c}{\partial\, {}^{t+\Delta t}T}\, ({}^{t+\Delta t}T - {}^{t}T)\, \boldsymbol{N}^{(e)}\, d\Omega \\
{}^{t+\Delta t}\boldsymbol{E}^{(e)} &= \frac{\partial(\sum_{i=1}^{n_c}\, {}^{t+\Delta t}F_{c_i}^{(e)})}{\partial\, {}^{t+\Delta t}\boldsymbol{T}^{(e)}} + \int_{\Omega^{(e)}} \boldsymbol{N}^{(e)\mathcal{T}}\, \rho_o\, \frac{\partial\, {}^{t+\Delta t}r}{\partial\, {}^{t+\Delta t}T}\; \boldsymbol{N}^{(e)}\, d\Omega + \\
&\quad + \int_{\Gamma_q^{(e)}} \boldsymbol{N}^{(e)\mathcal{T}}\, \frac{\partial\, {}^{t+\Delta t}\bar{q}}{\partial\, {}^{t+\Delta t}T}\; \boldsymbol{N}^{(e)}\, d\Gamma_q + \int_{\Gamma_q^{(e)}} \boldsymbol{N}^{(e)\mathcal{T}}\, \frac{\partial\, ({}^{t+\Delta t}h\; {}^{t+\Delta t}T_{env})}{\partial\, {}^{t+\Delta t}T}\; \boldsymbol{N}^{(e)}\, d\Gamma_q
\end{aligned}
$$

For numerical stability conditions a more convenient form of evaluating this derivative is:

$$
\left.\frac{\partial\, {}^{t+\Delta t}f_{pc}}{\partial\, {}^{t+\Delta t}T}\right|^{j} = \frac{{}^{t+\Delta t}f_{pc}^{j} - {}^{t}f_{pc}}{{}^{t+\Delta t}T^{j} - {}^{t}T}. \tag{4.7}
$$

Neglecting the "td" and external actions contributions in equation (4.5), and considering equation (4.7) for the temperature derivative of f_{pc}, the Jacobian matrix takes the simpler form:

$$
{}^{t+\Delta t}\boldsymbol{J}^{j} \simeq {}^{t+\Delta t}\bar{\boldsymbol{J}}^{j} = {}^{t+\Delta t}\boldsymbol{K}^{j} + \frac{{}^{t+\Delta t}\boldsymbol{C}^{j}}{\Delta t} + \frac{{}^{t+\Delta t}\boldsymbol{C}_{pc}^{j}}{\Delta t}. \tag{4.8}
$$

Obviously, $\bar{\boldsymbol{J}}$ is an approximate tangent Jacobian matrix and, therefore, the quadratic convergence of Newton-Raphson's method is lost. However, when solving the system of non-linear equations, the residual $\boldsymbol{R}$ is evaluated "exactly" (within the numerical frame) via equation (3.16). Consequently, this formulation is conservative in the weak form sense.

As f_{pc} can present a jump discontinuity inside an element in the isothermal case, a non-standard spatial integration is needed to compute $\boldsymbol{L}$ accurately.

Many researchers [42,43,45] have developed special integration techniques based in splitting the integral over $\Omega^{(e)}$ into $\Omega_s^{(e)}$ and $\Omega_l^{(e)}$ integrals, such that f_{pc} is a continuous function of T within those regions. Then, the standard Gaussian quadrature can be applied in each domain separately.

In the non-isothermal problem, the idea used in this paper is basically the same as described above but splitting the $\Omega^{(e)}$ integral into $\Omega_{n_{div}}^{(e)}$ integrals (with the number of element subdivisions n_{div} fixed). Although f_{pc} is continuous in $\Omega^{(e)}$ (but with great variations, depending on the size of the phase-change interval $(T_l - T_s)$), a more accurate integration is achieved using this subdomain technique.

Due to latent heat effects, a severe non-linearity is introduced in this problem. To take this fact into account, a proper convergence criterion for stopping the iteration process has to be used. The option used in this paper [42,43] is written as:

$$\frac{\|^{t+\Delta t}\boldsymbol{R}^j\|_2}{\|^{t+\Delta t}\boldsymbol{K}^j\ {}^{t+\Delta t}\boldsymbol{T}^j\|_2} < \epsilon_R \ , \tag{4.9}$$

where $\|.\|_2$ is the L_2 vector norm, and ϵ_R is the measure of the admissible out-of-balance residual (often taken equal to 10^{-3}).

5. COMPARISON WITH OTHER FINITE ELEMENT TECHNIQUES.

Different formulations within the framework of fixed-domain methods for solving phase-change problems have been developed by many researchers in recent years. The aim of this Section is to perform a brief comparative analysis between some of these techniques [20–35] and the temperature-based formulation presented above.

5.1. Enthalpy method.

Although there are different versions of this method, all of them define a new variable H, called the enthalpy, as [20]:

$$\tilde{c} = \frac{\partial H}{\partial T} = c + L\,\frac{\partial f_{pc}}{\partial T} \ , \tag{5.1}$$

where $\tilde{c}$ is the equivalent specific heat capacity. Note that in fact the enthalpy variable coincides with the specific internal energy as defined by equation (2.16).

In particular, one of such versions [20] retains the temperature as the nodal unknown variable while the enthalpy, computed using the exact $H-T$ curve (see ***Figure*** 3), is only needed to take into account the latent heat effect via equation (5.1) [20]. Substituting the equivalent specific heat capacity $\tilde{c}$ (equation (5.1)) into the generalized phase-change equation (3.8) and following the same procedure described in Section 3, the residual vector can be computed in this case as [20]:

$${}^{t+\Delta t}\tilde{\boldsymbol{R}} = {}^{t+\Delta t}\boldsymbol{F} - \left[\frac{{}^{t+\Delta t}\tilde{\boldsymbol{C}}}{\Delta t} + {}^{t+\Delta t}\boldsymbol{K}\right] {}^{t+\Delta t}\boldsymbol{T} + \frac{{}^{t+\Delta t}\tilde{\boldsymbol{C}}}{\Delta t}\ {}^{t}\boldsymbol{T} = \boldsymbol{0} \ , \tag{5.2}$$

where the element contribution of ${}^{t+\Delta t}\tilde{\boldsymbol{C}}$ is:

$${}^{t+\Delta t}\tilde{\boldsymbol{C}}^{(e)} = \int_{\Omega^{(e)}} \boldsymbol{N}^{(e)\mathcal{T}}\ {}^{t+\Delta t}\tilde{c}\ \boldsymbol{N}^{(e)}\ d\Omega. \tag{5.3}$$

Several approximated forms have been proposed to evaluate $\tilde{c}$ when phase-change occurs (see References [9 – 13]). However, due to numerical stability conditions [20], a regularization in the $H-T$ curve is necessary for the isothermal problem (see *Figure* 4).

It should be noted that equation (5.2) involves a temperature derivative of an almost (due to the regularization) discontinuous enthalpy function, because it derives from the integral equation (3.8) and not from (3.6). Clearly, equations (5.1) and (5.2) lead to an approximated evaluation of $\tilde{c}$ and $\tilde{\boldsymbol{R}}$, respectively. This fact makes the method to be non-conservative in

the weak form sense. Nevertheless, this drawback can be partially overcome if very small time steps are used.

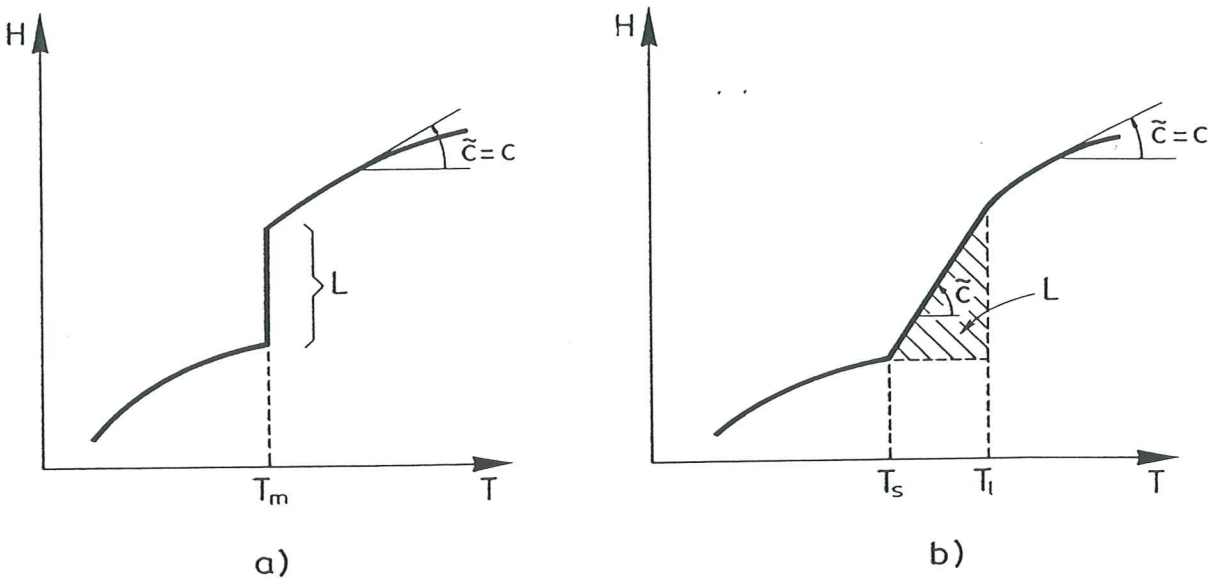

Figure 3. Exact enthalpy-temperature curve for phase-change problems: a) isothermal case. b) non-isothermal case.

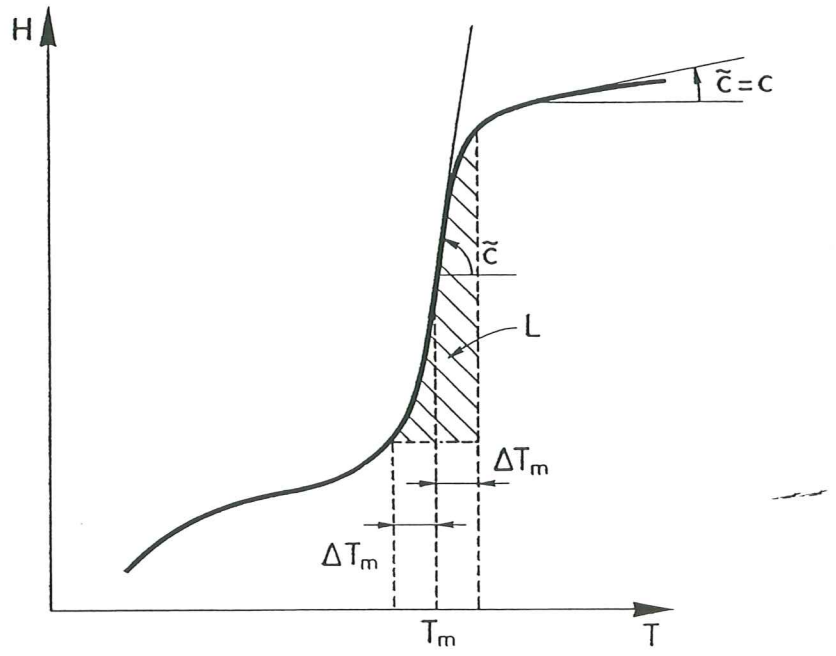

Figure 4. Regularized enthalpy-temperature curve for the isothermal phase-change problem (ΔT_m = regularization temperature interval).

As $\tilde{R}$ is computed approximately, it is not useful to derive an "exact" tangent Jacobian matrix and then is usually taken in this case simply as [20]:

$$^{t+\Delta t}\tilde{J} = {}^{t+\Delta t}K + \frac{^{t+\Delta t}\tilde{C}}{\Delta t}. \qquad (5.4)$$

A modification to recover improved nodal temperatures using the exact $H - T$ curve (or the regularized form used for the isothermal case), after computing H via the numerical integration of equation (5.1), has been proposed in [29]: However, in this case the residual vector is calculated as described above with the inherent drawbacks mentioned.

An alternative formulation considers the nodal enthalpies as the unknowns of the problem. For this purpose, the standard spatial interpolation is now adopted for H, i.e.:

$$H(\boldsymbol{x}) = \boldsymbol{N}(\boldsymbol{x})\, \boldsymbol{H}\ , \qquad (5.5)$$

with $\boldsymbol{H}$ being the nodal enthalpy vector. Furthermore, the following Taylor expansion is used [31]:

$$^{t+\Delta t}\boldsymbol{T} - {}^{t}\boldsymbol{T} = \frac{\partial\, ^{t+\Delta t}\boldsymbol{T}}{\partial\, ^{t+\Delta t}\boldsymbol{H}} \left(^{t+\Delta t}\boldsymbol{H} - {}^{t}\boldsymbol{H}\right) = {}^{t+\Delta t}\tilde{\boldsymbol{B}}\, \left(^{t+\Delta t}\boldsymbol{H} - {}^{t}\boldsymbol{H}\right)\ , \qquad (5.6)$$

where in general $\tilde{\boldsymbol{B}}$ is a full matrix. In practice, however, it is assumed to be a diagonal matrix containing the enthalpy derivative of the temperature at each node. Taking into account (3.8), (5.1) and (5.6) the residual is written as [31]:

$$^{t+\Delta t}\tilde{\boldsymbol{R}} = {}^{t+\Delta t}\boldsymbol{F} - \left[\frac{^{t+\Delta t}\boldsymbol{M}}{\Delta t} + {}^{t+\Delta t}\boldsymbol{K}\, {}^{t+\Delta t}\tilde{\boldsymbol{B}}\right] \left(^{t+\Delta t}\boldsymbol{H} - {}^{t}\boldsymbol{H}\right) - {}^{t+\Delta t}\boldsymbol{K}\, {}^{t}\boldsymbol{T} = \boldsymbol{0}\ , \qquad (5.7)$$

where $\boldsymbol{M}$ is the usual mass matrix. Due to the diagonalization of $\tilde{\boldsymbol{B}}$, the residual vector is computed in an approximated form. After solving the non-linear system of equations, the nodal temperature vector is evaluated by means of the "exact" $H - T$ curve. As it can be observed, this technique has the same drawbacks discussed above.

In this case, the simplified Jacobian matrix is taken as [31]:

$$^{t+\Delta t}\tilde{\boldsymbol{J}} = \frac{^{t+\Delta t}\boldsymbol{M}}{\Delta t} + {}^{t+\Delta t}\boldsymbol{K}\, {}^{t+\Delta t}\tilde{\boldsymbol{B}}. \qquad (5.8)$$

Note that both equations (5.4) and (5.8) incorporate the latent heat effect into the Jacobian matrix. This is important to avoid numerical oscillations when phase-change takes place.

To the authors' knowledge, no enthalpy method evaluates the residual vector as equation (3.16) does. Therefore, all these methods are only nearly conservative in the weak form sense.

5.2. Source method.

Rolph III and Bathe [35] include the non-linear effects due to phase-change in the residual as a source term $\tilde{\boldsymbol{Q}}$. The residual takes in this case the following form:

$$^{t+\Delta t}\tilde{\boldsymbol{R}} = {}^{t+\Delta t}\boldsymbol{F} - \left[\frac{^{t+\Delta t}\boldsymbol{C}}{\Delta t} + {}^{t+\Delta t}\boldsymbol{K}\right] {}^{t+\Delta t}\boldsymbol{T} + \frac{^{t+\Delta t}\boldsymbol{C}}{\Delta t}\, {}^{t}\boldsymbol{T} - {}^{t+\Delta t}\tilde{\boldsymbol{Q}} = \boldsymbol{0}. \qquad (5.9)$$

When computing $\tilde{\boldsymbol{Q}}$, some internal constraints are imposed in order to enforce the nodal temperature vector to follow the exact $H - T$ curve consistently with the amount of latent

heat released or absorbed. In fact, the moving interface condition is violated because an artificial (numerical) plateaux, leading to the impossible situation of zero interface velocity, is produced.

The proposed Jacobian matrix in this case is [35]:

$$^{t+\Delta t}\tilde{J} = {}^{t+\Delta t}K_{\cdot} \qquad (5.10)$$

It should be noted that now the latent heat effect is not considered in $\tilde{J}$.

Once more, the method is only nearly conservative in the weak form sense.

5.3. Temperature-based methods.

An important feature of these methods, which do not need any additional state variable for the numerical solution of the problem, is that the residual vector is evaluated using equation (3.16) (which derives from the integral equation (3.6)) with the consequence of being conservative in the weak form sense. Nevertheless, the most difficult task consists in finding an accurate Jacobian matrix which ensures convergence and stability of the algorithm.

In the frame of Quasi-Newton methods, Crivelli et al. [42] have proposed a Jacobian matrix of the form:

$$^{t+\Delta t}\tilde{J} = {}^{t+\Delta t}K + \frac{^{t+\Delta t}C}{\Delta t} + \frac{^{t+\Delta t}C_{T-B}}{\Delta t}\,, \qquad (5.11)$$

where C_{T-B} is a diagonal matrix computed at nodal level which takes into account phase-change effects. It has to be noted that this equation looks like equation (4.8). In fact, most temperature-based methods differ only in the evaluation procedure for C_{T-B}.

Later, Storti et al. [44] have derived a Jacobian matrix (considering constant thermal properties) exclusively for the isothermal problem. Its expression is similar to equation (5.11), but in this case the C_{T-B} contribution only exists for those elements containing the moving interface. However, convergence shortcomings reported by the authors appear in some limiting cases.

In the temperature-based formulation presented in previous Sections, the consistent Jacobian matrix is computed at Gauss point level and its contribution is detected in all the elements that have experienced the phase-change effect during the time increment for which equation (4.7) is used for the temperature derivative of f_{pc}. This fact makes the algorithm to be stable even in the isothermal case. It should be noted that this is not the case if equation (4.6) is considered.

In other words, the evaluation of the temperature derivative of f_{pc} via equation (4.7) ensures numerical stability and a reasonable convergence rate.

6. NUMERICAL EXAMPLES.

a) Example 1.

A 1-D example studied in References [35, 42] has been considered here. A semi-infinite slab initially in liquid state ($T_o(x) = 0\ ^oC$) is frozen with a imposed boundary condition at $x = 0$ ($T(0,t) = -45\ ^oC$). The analysis has been performed with 32 equally spaced linear two node

isoparametric elements of 0.125 m width. The thermal properties are found in *Table* 1. The time step used was 0.2 s. The temperature evolution of a point placed at $x = 1$ m is plotted in *Figure* 5. *Figure* 6 shows the front position evolution during the process.

b) Example 2.

A two-dimensional example is also analyzed [1,43]. A semi-infinite skew region, initially at 0.3 ^oC, is frozen by lowering the temperature on the side $y = 0$ to -1 ^oC. The geometry and the finite element mesh used are plotted in *Figure* 7. Four node bilinear isoparametric elements have been used in the computations. The thermal properties are given in *Table* 2. Since the problem is symmetric along the line $x = y$, the analysis is rectricted to the region $y \geq 0$ and $x \geq y$, imposing adiabatic conditions on the mentioned line. To simulate the infinite region, adiabatic conditions have been also imposed on the other two boundaries. Using a time step of 0.01 s, two temperature profiles along the line $x = y$ for $t = 0.04$ s and $t = 0.08$ s are shown in *Figures* 8 and 9 respectively. *Figure* 10 depicts the front position evolution along the same line $x = y$.

As it can be observed, a very good agreement between analytical and numerical results is achieved in both examples.

CONCLUSIONS.

A temperature-based finite element formulation has been presented. The main features of such a formulation are:

- it is conservative in the weak form sense,
- it preserves the moving interface condition,
- it can solve generalized phase-change problems,
- it does not need any explicit regularization because an accurate integration technique is employed. Thus, coarser meshes and larger time steps (in comparison with other methods) can be used,
- it considers a proper convergence criterion,
- a consistent Jacobian matrix has been derived. This ensures numerical stability and a reasonable convergence rate,
- the numerical examples analyzed show the accuracy of the present formulation and its computational efficiency.

Although a rigorous convergence and stability analyses are still lacking, numerical experiments have demonstrated that the present formulation is robust and it can accurately simulate generalized phase-change problems.

ACKNOWLEDGEMENTS.

This work has been supported by RENAULT, under contract nº CIMNE/10/H5.12.603. The support provided by BRITE/EURAM Project nº BE-4596 under contract nº BREU-0443 is also gratefully acknowledged.

REFERENCES.

[1]- **Budhia H. and Kreith F.** - Heat Transfer with Melting or Freezing in a Wedge -*Int. J. Heat Mass Transfer, Vol. 16, pp. 195-211 (1973).*

[2]- **Tao L.** - The Stefan Problem with an Imperfect Thermal Contact at the Interface -*Journal of Applied Mechanics, December 1982, Vol. 49 (715-720).*

[3]- **Lazaridis A.** - A Numerical Solution of the Multidimensional Solidification (or Melting) Problem -*Int. J. Heat Mass Transfer, Vol. 13, pp. 1459-1477 (1970).*

[4]- **Shamsundar N. and Sparrow E.** - Analysis of Multidimensional Conduction Phase Change Via the Enthalpy Model -*Journal of Heat Transfer, August 1975 (333-340).*

[5]- **Goodrich L.** - Efficient Numerical Technique for One-Dimensional Thermal Problems with Phase Change -*Int. J. Heat Mass Transfer, Vol. 21, pp. 615-621 (1978).*

[6]- **Bell G. and Wood A.** - On the Performance of the Enthalpy Method in the Region of a Singularity -*Int. Jour. Num. Meth. Engng., Vol. 19, 1583-1592 (1983).*

[7]- **O'Neill K.** - Boundary Integral Equation Solution of Moving Boundary Phase Change Problems -*Int. Jour. Num. Meth. Engng., Vol. 19, 1825-1850 (1983).*

[8]- **Zabaras N. and Mukherjee S.** - An Analysis of Solidification Problems by the Boundary Element Method -*Int. Jour. Num. Meth. Engng., Vol. 24, 1879-1900 (1987).*

[9]- **Salcudean M. and Abdullah Z.** - On the Numerical Modelling of Heat Transfer During Solidification -*Int. Jour. Num. Meth. Engng., Vol. 25, 445-473 (1988).*

[10]- **Tamma, K. and Namburu R.** - Recent Advances, Trends and New Perspectives Via Enthalpy-Based Finite Element Formulations for Applications to Solidification Problems -*Int. Jour. Num. Meth. Engng., Vol. 30, 803-820 (1990).*

[11]- **Voller V., Swaminathan C. and Thomas B.** - Fixed Grid Techniques for Phase Change Problems: a Review -*Int. Jour. Num. Meth. Engng., Vol. 30, 875-898 (1990).*

[12]- **Dalhuijsen A. and Segal A.** - Comparison of Finite Element Techniques for Solidification Problems -*Int. Jour. Num. Meth. Engng., Vol. 23, 1807-1829 (1986).*

[13]- **Viskanta R.** - Heat Transfer During Melting and Solidification of Metals -*J. Heat Transfer ASME, 110, 1205-1219 (1988).*

[14]- **Lynch D. and O'Neill K.** - Continuously Deforming Finite Elements for the Solution of Parabolic Problems, With and Without Phase Change -*Int. Jour. Num. Meth. Engng., Vol. 17, 81-96 (1981).*

[15]- **Tacke K.** - Discretization of the Explicit Enthalpy Method for Planar Phase Change -*Int. Jour. Num. Meth. Engng., Vol. 21, 543-554 (1985).*

[16]- **Askar H.** - The Front-Tracking Scheme for the One-Dimensional Freezing Problem -*Int. Jour. Num. Meth. Engng., Vol. 24, 859-869 (1987).*

[17]- **Zabaras N. and Ruan Y.** - A Deforming Finite Element Method Analysis of Inverse Stefan Problems -*Int. Jour. Num. Meth. Engng., Vol. 28, 295-313 (1989).*

[18]- **Ruan Y. and Zabaras N.** - An Inverse Finite-Element Technique to Determine the Change of Phase Interface Location in Two-Dimensional Melting Problems -*Comm. Appl. Numer. Meth., Vol. 7, 325-338 (1991).*

[19]- **Bénard C. and Afshari A.** - Inverse Stefan Problem: Tracking of the Interface Position from Measurements of the Solid Phase -*Int. Jour. Num. Meth. Engng., Vol. 35, 835-851 (1992).*

[20]- **Voller V. and Cross M.** - Accurate Solutions of Moving Boundary Problems Using

the Enthalpy Method -*Int. J. Heat Mass Transfer, Vol. 24, pp. 545-556 (1981).*

[21]- **Bonacina C., Comini G., Fasano A. and Primicerio M.** - Numerical Solution of Phase-Change Problems -*Int. J. Heat Mass Transfer, Vol. 16, pp. 1825-1832 (1973).*

[22]- **Bell G.** - On the Performance of the Enthalpy Method -*Int. J. Heat Mass Transfer, Vol. 25, pp. 587-589 (1982).*

[23]- **Wood A., Ritchie S. and Bell G.** - An Efficient Implementation of the Enthalpy Method -*Int. Jour. Num. Meth. Engng., Vol. 17, 301-305 (1981).*

[24]- **Desbiolles J., Droux J., Rappaz J. and Rappaz M.** - Simulation of Solidification of Alloys by the Finite Element Method -*Computer Physics Reports 6 (1987) 371-383. North Holland, Amsterdam.*

[25]- **Lewis R. and Roberts P.** - Finite Element Simulation of Solidification Problems -*Applied Scientific Research 44: 61-92 (1987). Martinus Nijhoff Publishers.*

[26]- **Hibbitt H. and Marcal P.** - Numerical Thermo-mechanical Model for the Welding and Subsequent Loading of a Fabricated Structure -*Comp. Struct., 3, 1145-1174 (1973).*

[27]- **Morgan K., Lewis R. and Zienkiewicz O.** - An Improved Algorithm for Heat Convection Problems with Phase Change -*Int. Jour. Num. Meth. Engng., Vol. 12, 1191-1195 (1978).*

[28]- **Comini, G., Del Guidice S, Lewis, R. and Zienkiewicz, O.** - Finite Element Solution of Non-Linear Heat Conduction Problems with Special Reference to Phase Change -*Int. Jour. Num. Meth. Engng., Vol. 8, 613-624 (1974).*

[29]- **Comini, G., Del Guidice S. and Saro O.** - A Conservative Algorithm for Multidimensional Conduction Phase Change -*Int. Jour. Num. Meth. Engng., Vol. 30, 697-709 (1990).*

[30]- **Droux J.** - Three-Dimensional Numerical Simulation of Solidification by an Improved Explicit Scheme -*Comp. Meth. in App. Mech. and Engng., 85 (1991), 57-74.*

[31]- **Thévoz P., Desbiolles J. and Rappaz M.** - Modelling of Equiaxed Microstructure Formation in Casting -*Metallurgical Transactions A, Vol. 20A, February 1989 (311-322).*

[32]- **Naik H. and Dave K.** - Solidification of Castings in Metallic Moulds -*Comm. Appl. Mech., Vol. 5, 467-472 (1989).*

[33]- **Chidiac S., Samarasekera I. and Brimacombe J.** - A Numerical Method for Analysis of Phase Change in the Continuous Casting Process -*Nuniform 89 (121-128), Thompson et al. (eds), Balkema, Rotterdam.*

[34]- **Voller V., Cross M. and Markatos N.** - An Enthalpy Method for Convection/Diffusion Phase Change -*Int. Jour. Num. Meth. Engng., Vol. 24, 271-284 (1987).*

[35]- **Rolph III, W. and Bathe K.** - An Efficient Algorithm for Analysis of Nonlinear Heat Transfer with Phase Changes -*Int. Jour. Num. Meth. Engng., Vol. 18, 119-134 (1982).*

[36]- **Roose J. and Storrer O.** - Modelization of Phase Changes by Fictitious Heat Flow -*Int. Jour. Num. Meth. Engng., Vol. 20, 217-225 (1984).*

[37]- **Reddy M. and Reddy J.** - Numerical Simulation of Forming Processes Using a Coupled Fluid Flow and Heat Transfer Model -*Int. Jour. Num. Meth. Engng., Vol. 35, 807-833 (1992).*

[38]- Blanchard D. and Fremond M. - The Stefan Problem: Computing Without the Free Boundary -*Int. Jour. Num. Meth. Engng., Vol. 20, 757-771 (1984).*

[39]- Ichikawa Y. and Kikuchi N. - A One-Phase Multi-Dimensional Stefan Problem by the

Method of Variational Inequalities -*Int. Jour. Num. Meth. Engng., Vol. 14, 1197-1220 (1979).*

[40]- **Lee T., Advani S., Lee J. and Moon H.** - A Fixed Grid Finite Element Method for Nonlinear Diffusion Problems with Moving Boundaries -*Computational Mechanics (1991) 8, 111-123.*

[41]- **Tamma K. and Railkar S.** - Hybrid Transfinite Element Modelling Analysis of Non-Linear Heat Conduction Problems Involving Phase Change -*Eng. Comput., 1988, Vol. 5, June (117-122).*

[42]- **Crivelli L. and Idelsohn S.** - A Temperature-based Finite Element Solution for Phase-Change Problems -*Int. Jour. Num. Meth. Engng., Vol. 23, 99-119 (1986).*

[43]- **Storti, M., Crivelli L. and Idelsohn S.** - Making Curved Interfaces Straight in Phase-Change Problems -*Int. Jour. Num. Meth. Engng., Vol. 24, 375-392 (1987).*

[44]- **Storti, M, Crivelli L. and Idelsohn S.** - An Efficient Tangent Scheme for Solving Phase-Change Problems -*Comp. Meth. in App. Mech. and Engng., 66 (1988), 65-86.*

[45]- **Steven G.** - Internally Discontinuous Finite Elements for Moving Interface Problems -*Int. Jour. Num. Meth. Engng., Vol. 18, 569-582 (1982).*

[46]- **Coleman B. and Gurtin M.** - Thermodynamics with Internal State Variables -*The Journal of Chemical Physics, Volume 47, Number 2, 15 July 1967.*

[47]- **Simo, J.** - Nonlinear Stability of the Time-Discrete Variational Problem of Evolution in Nonlinear Heat Conduction, Plasticity and Viscoplasticity -*Comp. Meth. in App. Mech. and Engng., 88 (1991), 111-131.*

[48]- **Lubliner J.** - On the Thermodynamics Foundations of Non-Linear Solid Mechanics -*Int. J. Non-linear Mechanics 7, 237-254 (1972).*

[49]- **Hughes T.** -*The Finite Element Method* - 1987, Prentice-Hall International, Inc.

[50]- **Malvern L.** -*Introduction to the Mechanics of a Continuous Medium* - 1969, Prentice-Hall, Inc.

[51]- **Celentano D.** -*Modelización por elementos finitos del enfriamiento de piezas de fundición* - Internal Repport (in Spanish), CIMNE Nº IT-28, Abril 1991.

[52]- **Celentano D., Oller S. and Oñate E.** -*A Constitutive Thermomechanical Model for Solidification of Metals* - Journées Numériques de Besançon: Les problemes de changement de phase, pp. 19-30, Septembre 1991.

[53]- **Celentano D., Oller S. and Oñate E.** -*A Plastic Constitutive Model to Simulate the Solidification in Casting Problems* - Proceedings of Complas III, pp. 1089-1102. R. Owen, E. Oñate and E. Hinton (Eds.). Pineridge Press/CIMNE, 1992.

[54]- **Celentano D.** -*A Thermomechanical Model for the Solidification of Metals* - Ph.D. Thesis (in course), U.P.C., Barcelona, Spain, 1992.

[55]- **Zienkiewicz O. and Taylor R.** -*The Finite Element Method* - 4th ed., Vol.1 & 2, McGraw-Hill, London, 1989.

Table 1

THERMAL PROPERTIES

- Specific heat capacity of the solid phase: $c = c_s = 1.0 \left[\frac{J}{Kg^oC}\right]$
- Specific heat capacity of the liquid phase: $c = c_l = 1.0 \left[\frac{J}{Kg^oC}\right]$
- Conductivity tensor of the solid phase: $k_{ij} = \delta_{ij} k_s;\ k_s = 1.08 \left[\frac{J}{ms^oC}\right]$
- Conductivity tensor of the liquid phase : $k_{ij} = \delta_{ij} k_l;\ k_l = 1.08 \left[\frac{J}{ms^oC}\right]$
- Density of the solid phase: $\rho_o = \rho_{o_s} = 1.0 \left[\frac{Kg}{m^3}\right]$
- Density of the liquid phase: $\rho_o = \rho_{o_l} = 1.0 \left[\frac{Kg}{m^3}\right]$
- Latent heat: $L = 70.26 \left[\frac{J}{Kg}\right]$
- Melting Temperature: $T_m = -1.0\ [^oC]$

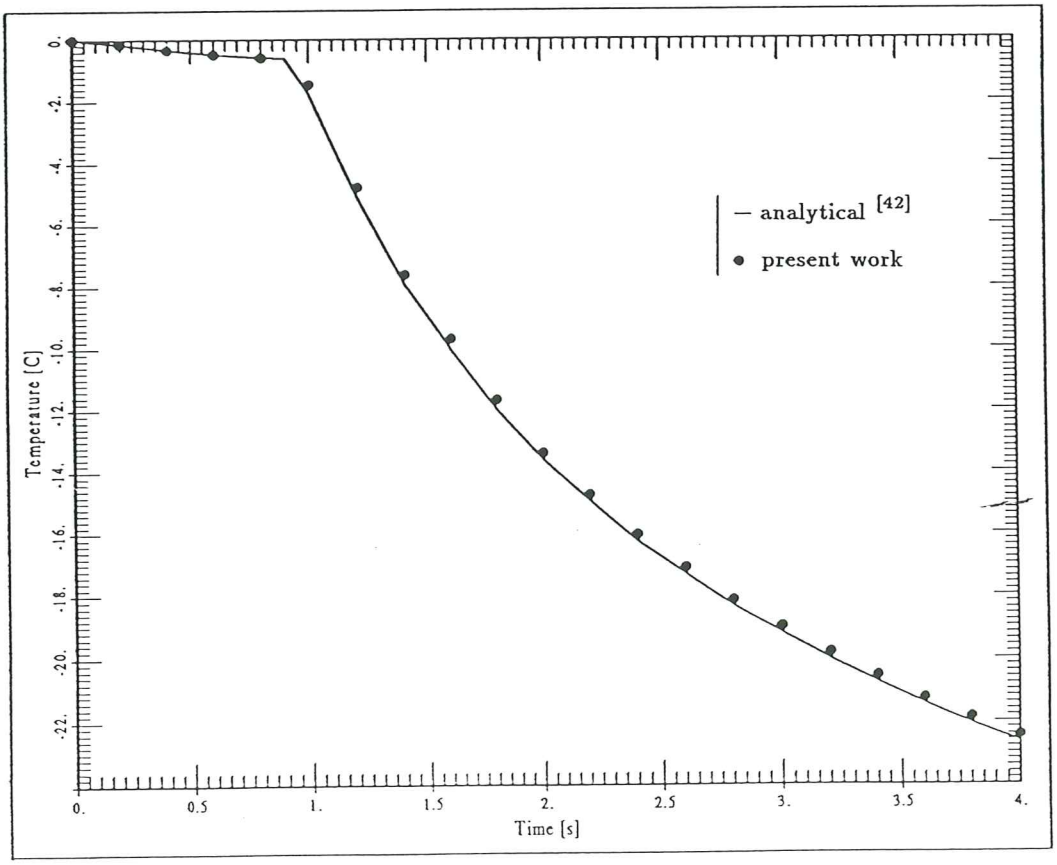

Figure 5. 1D Phase-change problem: temperature evolution at x=1 m.

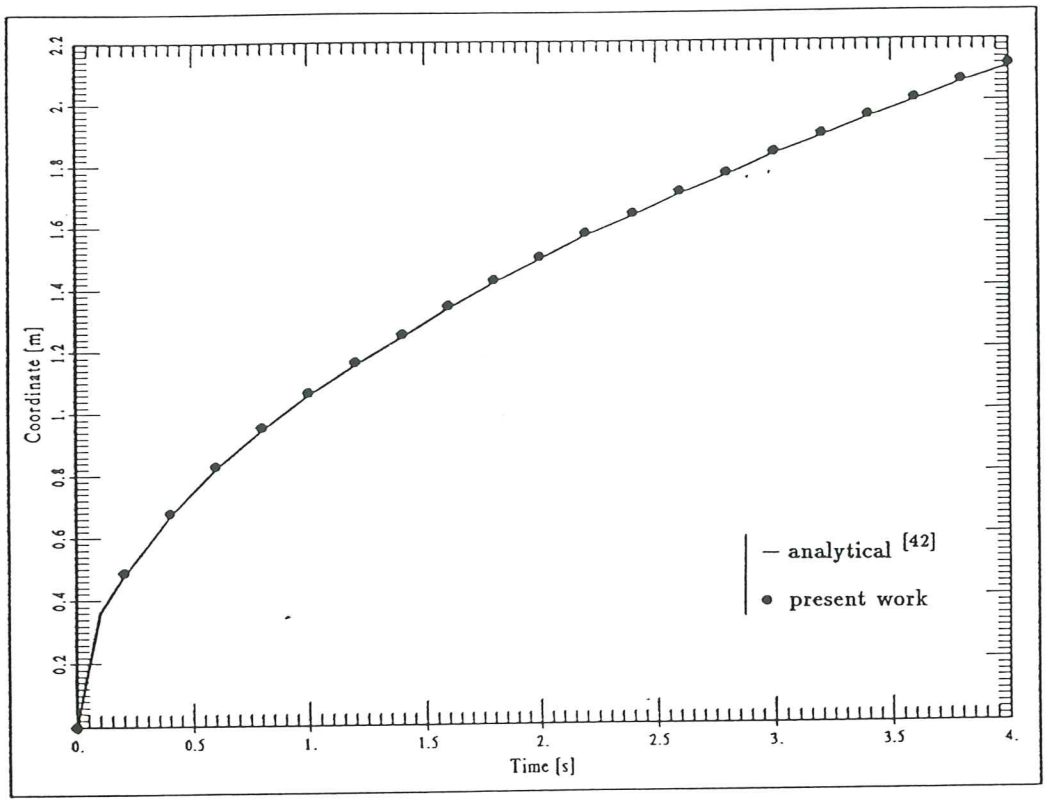

Figure 6. 1D Phase-change problem: front position evolution.

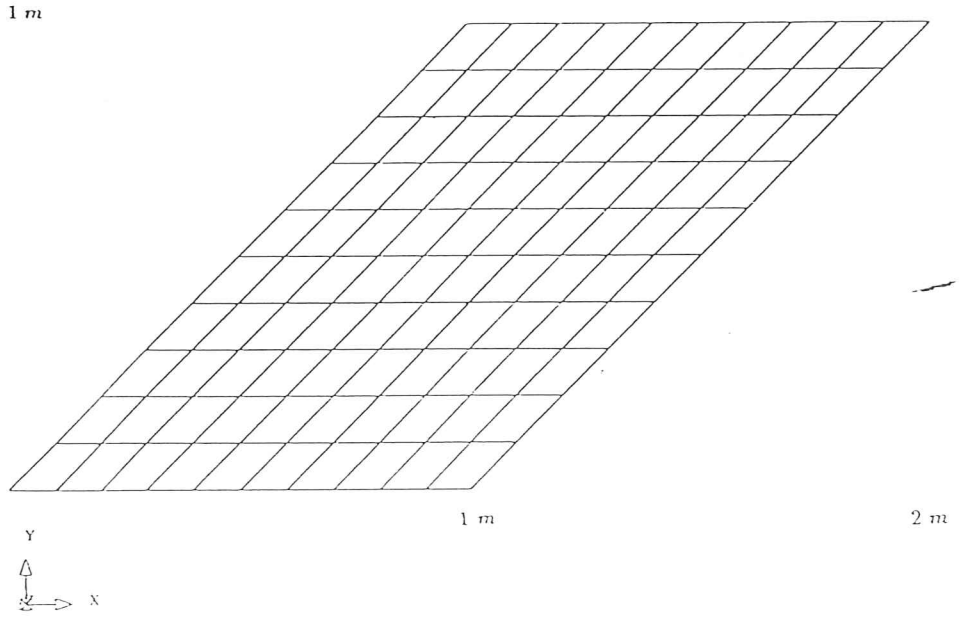

Figure 7. 2D Phase-change problem: geometry and finite element mesh.

Table 2

THERMAL PROPERTIES

- Specific heat capacity of the solid phase: $c = c_s = 1.0 \left[\frac{J}{Kg^oC}\right]$
- Specific heat capacity of the liquid phase: $c = c_l = 1.0 \left[\frac{J}{Kg^oC}\right]$
- Conductivity tensor of the solid phase: $k_{ij} = \delta_{ij} k_s;\ k_s = 1.0 \left[\frac{J}{ms^oC}\right]$
- Conductivity tensor of the liquid phase : $k_{ij} = \delta_{ij} k_l;\ k_l = 1.0 \left[\frac{J}{ms^oC}\right]$
- Density of the solid phase: $\rho_o = \rho_{o_s} = 1.0 \left[\frac{Kg}{m^3}\right]$
- Density of the liquid phase: $\rho_o = \rho_{o_l} = 1.0 \left[\frac{Kg}{m^3}\right]$
- Latent heat: $L = 0.25 \left[\frac{J}{Kg}\right]$
- Melting Temperature: $T_m = 0.0\ [^oC]$

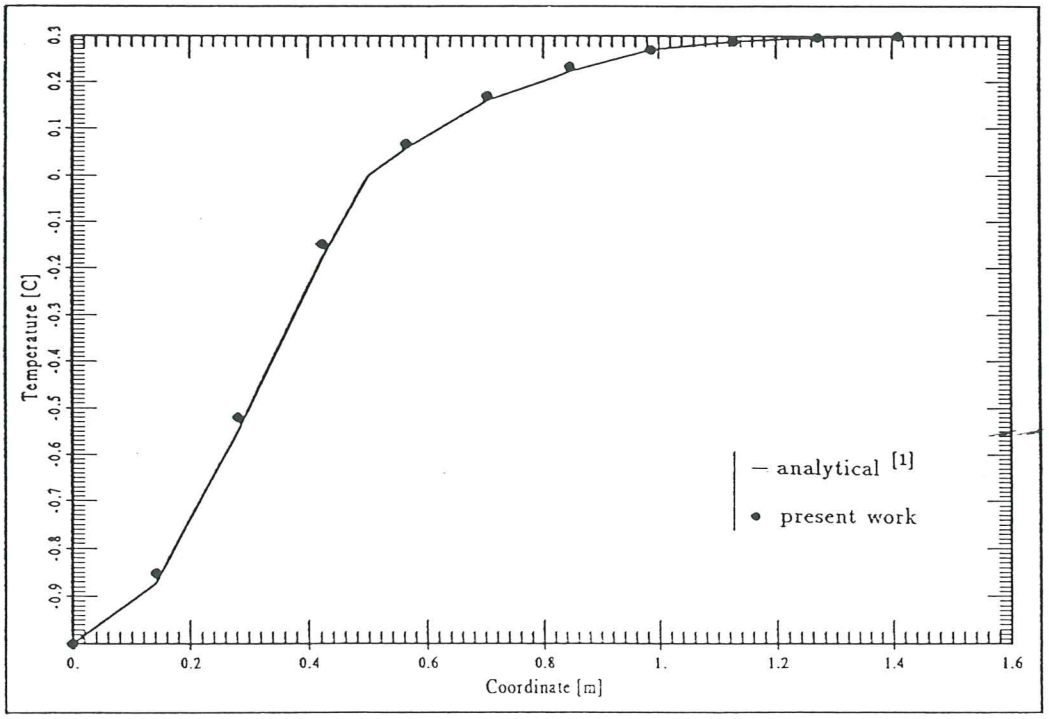

Figure 8. 2D Phase-change problem: temperature profile along x=y for t=0.04 s.

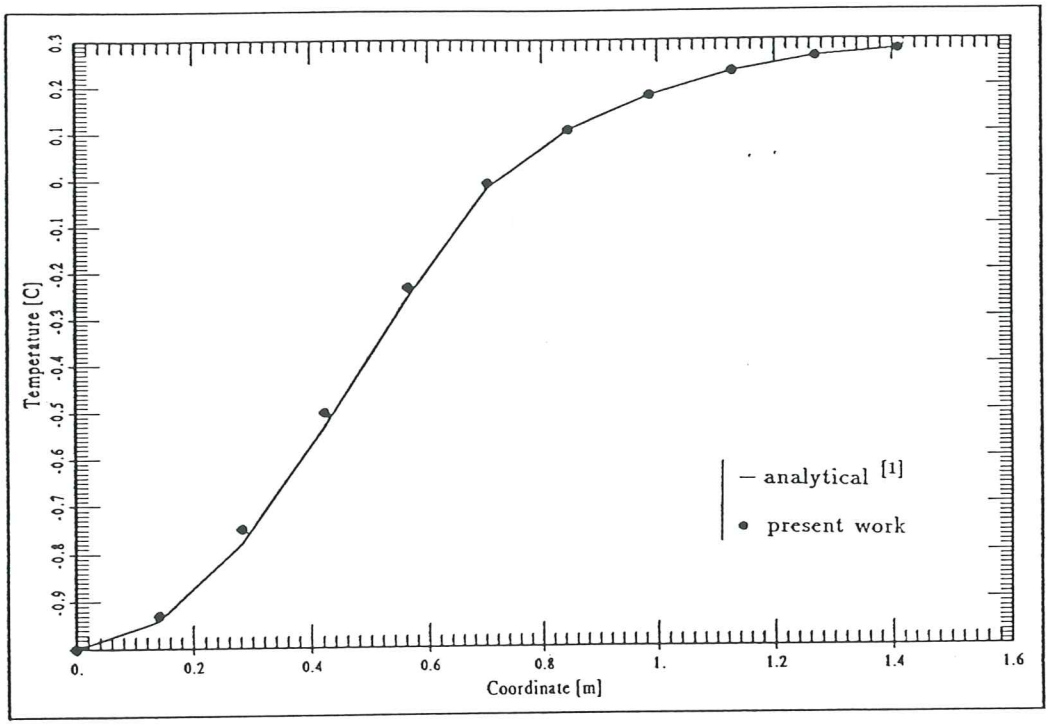

Figure 9. 2D Phase-change problem: temperature profile along x=y for t=0.08 s.

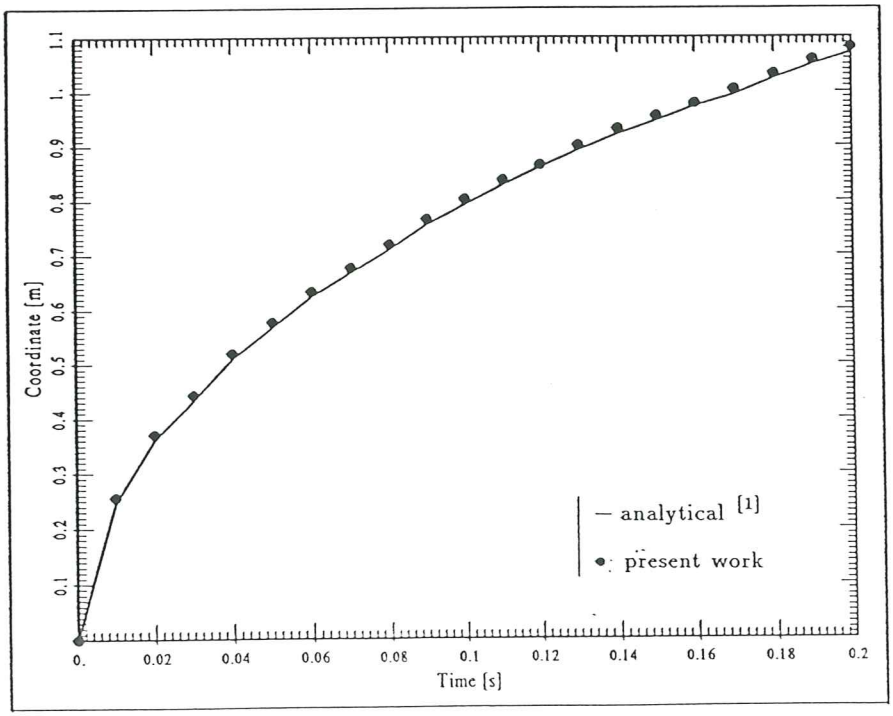

Figure 10. 2D Phase-change problem: front position evolution along x=y.